Journal of Pharmaceutical and Biomedical Analysis 47 (2008) 819–827

Contents lists available at ScienceDirect

Journal of Pharmaceutical and Biomedical Analysis

journal homepage: www.elsevier.com/locate/jpba

# Development of a method for the determination of caffeine anhydrate in various designed intact tables by near-infrared spectroscopy: A comparison between reflectance and transmittance technique

Masatomo Ito [a,*], Tatsuya Suzuki [a], Shuichi Yada [a], Akira Kusai [a], Hiroaki Nakagami [a], Etsuo Yonemochi [b], Katsuhide Terada [b]

[a] Formulation Technology Research Laboratories, Daiichi-Sankyo Co. Ltd., 1-12-1 Shinomiya, Hiratsuka, Kanagawa 254-0014, Japan
[b] School of Pharmaceutical Sciences, Toho University, 2-2-1 Miyama, Funabashi, Chiba 274-8510, Japan

ARTICLE INFO

*Article history:*
Received 1 November 2007
Received in revised form 12 February 2008
Accepted 28 March 2008
Available online 10 April 2008

*Keywords:*
Reflectance near-infrared spectroscopy
Transmittance near-infrared spectroscopy
Partial least-squares
Tablet design
Caffeine anhydrate

ABSTRACT

Using near-infrared (NIR) spectroscopy, an assay method which is not affected by such elements of tablet design as thickness, shape, embossing and scored line was developed. Tablets containing caffeine anhydrate were prepared by direct compression at various compression force levels using different shaped punches. NIR spectra were obtained from these intact tablets using the reflectance and transmittance techniques. A reference assay was performed by high-performance liquid chromatography (HPLC). Calibration models were generated by the partial least-squares (PLS) regression. Changes in the tablet thickness, shape, embossing and scored line caused NIR spectral changes in different ways, depending on the technique used. As a result, noticeable errors in drug content prediction occurred using calibration models generated according to the conventional method. On the other hand, when the various tablet design elements which caused the NIR spectral changes were included in the model, the prediction of the drug content in the tablets was scarcely affected by those elements when using either of the techniques. A comparison of these techniques resulted in higher predictability under the tablet design variations using the transmittance technique with preferable linearity and accuracy. This is probably attributed to the transmittance spectra which sensitively reflect the differences in tablet thickness or shape as a result of obtaining information inside the tablets.



## 1. Introduction

Recently, the concept of process analytical technology (PAT) was introduced in the FDA's Guidance for Industry [1]. PAT enables quality assurance of a whole batch by monitoring the critical-to-quality attributes (CQAs) during the manufacturing processes. As a PAT tool, near-infrared (NIR) spectroscopy is extensively used to monitor such CQAs as moisture content in the granules and crystal form of a drug during the granulating—drying process [2–7], compact hardness during the roller compaction process [8,9], blend uniformity during the powder blending process [10–18], lubricant uniformity during lubricating [19–21], tablet hardness during the tableting process [22] and film quantitation during the film coating process [23,24] because of its rapid and non-destructive process. NIR spectroscopy is also used for tablet content uniformity testing [25–29] and can be applied derivatively to monitor the drug content in each tablet during the tableting process.

In order to introduce PAT tools to production in a factory, it is necessary to identify the CQAs and to establish a monitoring method for the CQAs during the production process by the use of PAT tools during pharmaceutical development which includes formulation optimization. Since the NIR spectra are affected by the components and compositions of drug products, separate calibration models for uniquely different formulations are usually needed, and the development of separate calibration models is time-consuming. In order to overcome this problem, the establishment of formulation-independent calibration models is desired. Weiβner et al. reported the development of excipient-independent calibration models [30] and Li et al. reported the development of a calibration-free semi-quantitative method [31]. Optimization of the tablet design, including embossing and scored line, are also made during pharmaceutical development in order to reduce the risk of such troubles as tableting deficiency including capping in the tableting process, and abrasion in the coating process [32,33] and

* Corresponding author. Tel.: +81 463 31 6954; fax: +81 463 31 6475.
*E-mail address:* ito.masatomo.id@daiichisankyo.co.jp (M. Ito).

0731-7085/$ – see front matter © 2008 Elsevier B.V. All rights reserved.
doi:10.1016/j.jpba.2008.03.033

furthermore to allow discrimination between tablets of different strengths or rival products. As well, a scored line is applied to some tablets so that the dose can be easily divided in clinical practice. However, very few studies have been reported on the NIR spectral changes by different tablet designs and their effects on the results from NIR analysis.

NIR spectroscopic analysis of tablets is non-destructive and measures the absorption of irradiated light onto the tablet. Some of irradiated NIR light penetrates through the tablet following a straight path or a scattering path. After partially penetrating into the tablet, the irradiated NIR light may also reflect off the surface of the tablet by scattering. The NIR transmittance technique detects the light penetrated through the tablet, and the NIR reflectance technique detects the light reflected from the tablet. It is known that the packing conditions of a sample affect the propagation of the irradiated light in the sample, hence affecting the absorption of irradiated light due to Beer's law accounting for the proportional relationship of the path length to the absorption of irradiated light. The effect of the sample density on the light path was proposed by Tsuchikawa et al. using time-of-flight near-infrared spectroscopy by means of a relationship between the pore structure of the sample and the light transmittance of NIR [34,35]. The theory is as follows. Since a high porosity sample has a larger air/solid boundary surface area, the intensity of the scattered light is greater than that of the straight light in the sample. Conversely, since a tightly packed sample has a larger solid/solid boundary surface area, the intensity of the scattered light is less than that of the straight light. In fact, spectral shift resulting from changes in the tablet density has been reported [27,28]. As well, changes in the tablet shape probably affect its packing conditions and hence its light propagation, as well as changes in tablet surface shape, such as embossing and scored line, which may affect its reflected light.

From the point of view of measurement techniques, many studies on the comparison of the transmittance with the reflectance techniques in terms of accuracy have been made and the transmittance technique has shown higher accuracy [36,37]. These results may be derived from differences in the detecting volume of the tablets, that is, the detecting volume using the transmittance technique is larger than that using the reflectance technique, which analyzes only the tablet's surface layer [38]. These previous studies were conducted with fixed tablet designs. However, taking various tablet designs into account, it is not necessarily appropriate to suggest that the accuracy using the transmittance technique is higher.

The purpose of the present work is to develop an assay method which is readily applicable to various designed tablets using only one calibration model. In this paper, the effect of such elements of tablet design as thickness, shape (round), embossing and scored line on the NIR spectra and drug content measurement by NIR spectroscopy using the reflectance or transmittance technique was investigated. In addition, the prediction accuracy of the transmittance technique was compared with that of the reflectance technique and the reason for their difference in accuracy was discussed. Tablets containing caffeine anhydrate as an active pharmaceutical ingredient (API) at various concentrations were prepared by direct compression. To obtain various designed tablets, the tablets were compressed at various compression force levels with different shaped punches. Their NIR spectra were measured by the reflectance or transmittance technique. High-performance liquid chromatography (HPLC) was used as a reference method. Cal-

**Table 1**
Formulation, compaction pressure, and shape of tablets for the calibration set and prediction set

| Batch no. | CAF (mg per tablet) | MCC (mg per tablet) | C-Na (mg per tablet) | Mg-St (mg per tablet) | Pressure (kN) | Tablet shape |
|---|---|---|---|---|---|---|
| For calibration set | | | | | | |
| 1 | 90 | 201 | 6 | 3 | 9.0 | Flat faced |
| 2 | 96 | 195 | 6 | 3 | 9.0 | Flat faced |
| 3 | 102 | 189 | 6 | 3 | 9.0 | Flat faced |
| 4 | 108 | 183 | 6 | 3 | 9.0 | Flat faced |
| 5 | 114 | 177 | 6 | 3 | 9.0 | Flat faced |
| 6 | 120 | 171 | 6 | 3 | 9.0 | Flat faced |
| 7 | 126 | 165 | 6 | 3 | 9.0 | Flat faced |
| 8 | 132 | 159 | 6 | 3 | 9.0 | Flat faced |
| 9 | 138 | 153 | 6 | 3 | 9.0 | Flat faced |
| 10 | 96 | 195 | 6 | 3 | 6.5 | Flat faced |
| 11 | 96 | 195 | 6 | 3 | 11.5 | Flat faced |
| 12 | 96 | 195 | 6 | 3 | 14.0 | Flat faced |
| 13 | 96 | 195 | 6 | 3 | 16.5 | Flat faced |
| 14 | 114 | 177 | 6 | 3 | 6.5 | Flat faced |
| 15 | 114 | 177 | 6 | 3 | 11.5 | Flat faced |
| 16 | 114 | 177 | 6 | 3 | 14.0 | Flat faced |
| 17 | 114 | 177 | 6 | 3 | 16.5 | Flat faced |
| 18 | 132 | 159 | 6 | 3 | 6.5 | Flat faced |
| 19 | 132 | 159 | 6 | 3 | 11.5 | Flat faced |
| 20 | 132 | 159 | 6 | 3 | 14.0 | Flat faced |
| 21 | 132 | 159 | 6 | 3 | 16.5 | Flat faced |
| 22 | 96 | 195 | 6 | 3 | 9.0 | Flat beveled edge |
| 23 | 114 | 177 | 6 | 3 | 9.0 | Flat beveled edge |
| 24 | 132 | 159 | 6 | 3 | 9.0 | Flat beveled edge |
| 25 | 96 | 195 | 6 | 3 | 9.0 | Convex |
| 26 | 114 | 177 | 6 | 3 | 9.0 | Convex |
| 27 | 132 | 159 | 6 | 3 | 9.0 | Convex |
| For prediction set | | | | | | |
| 28 | 120 | 171 | 6 | 3 | 6.5 | Flat faced |
| 29 | 120 | 171 | 6 | 3 | 11.5 | Flat faced |
| 30 | 120 | 171 | 6 | 3 | 9 | Flat beveled edge |
| 31 | 120 | 171 | 6 | 3 | 9 | Convex |
| 32 | 120 | 171 | 6 | 3 | 9 | Flat faced |

CAF: caffeine anhydrate, MCC: microcrystalline cellulose, C-Na: croscarmellose sodium, Mg-St: magnesium stearate.

ibration models were generated by the partial least-squares (PLS) method followed by leave-one-out cross-validations. These calibration models were used to predict the drug content in the tablets made for model validation.

## 2. Materials and methods

### 2.1. Materials

Caffeine anhydrate was purchased from Shiratori Pharmaceutical Co. Ltd. (Chiba, Japan). Microcrystalline cellulose (Ceolus PH102) was purchased from Asahi Kasei Chemicals Corporation (Tokyo, Japan). Croscarmellose sodium (Ac-Di-Sol) was purchased from Kaneda Corporation (Tokyo, Japan). Magnesium stearate was purchased from Tyco Healthcare (Tokyo, Japan). Each of these was used as received in the following study. All other reagents were of analytical grade and were used without further purification.

### 2.2. Tablet preparation

Tablets containing caffeine anhydrate as an active pharmaceutical ingredient with strength in the range of 90–138 mg, microcrystalline cellulose, croscarmellose sodium, and magnesium stearate were prepared by direct compression. The formulation, compression force, and shape of tablets are summarized in Table 1. In detail, caffeine anhydrate, microcrystalline cellulose, and croscarmellose sodium were mixed using a convection mixer (KC-HUK type, Konishi Medical Instruments Co. Ltd., Japan) at 10,000 rpm for 1 min. The amount of microcrystalline cellulose was adjusted to give a final weight for each tablet of approximately 300 mg, as shown in Table 1. Subsequently, magnesium stearate was added to the mixture, which was mixed in a plastic bag to make tableting powders. A total of 300 mg of this tableting powder was filled in a die (Ø 9.5 mm) and then compressed using an oil press and flat-faced punches. To prepare tablets in various thicknesses, various compression forces were applied to the tablets. Different shaped punches were also used to prepare flat beveled edge tablets with embossing and a scored line on one side or convex tablets with embossing on one side (Fig. 1). The number of samples included three for each calibration batch and five for each prediction batch. The tablet thicknesses were measured using a dial thickness gauge (SM-112, Teclock, Japan).

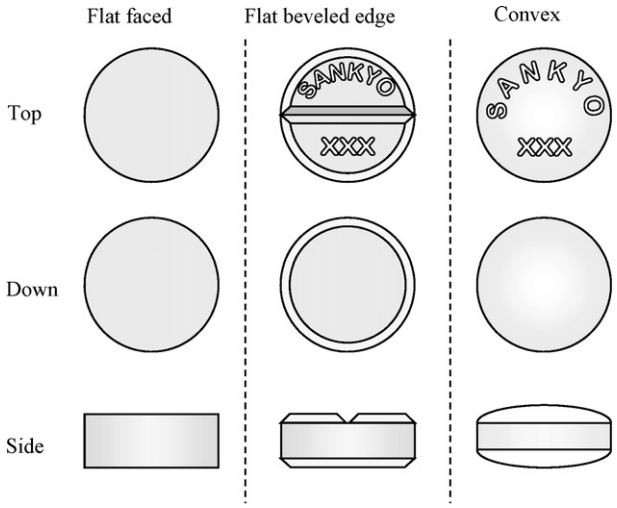


**Fig. 1.** Illustrations of various designed tablets used in this study.

### 2.3. NIR spectroscopic analysis

The prepared tablet samples were first analyzed using an XDS Rapid Content Analyzer (RCA) (Foss NIRSystems Inc., Laurel, MD, USA). The RCA was operated in the diffuse reflectance mode. A tablet holder which closely fits the contour of the tablets was used to fix the position of the tablet on the instrument. Upon reaching the sample, the irradiated light penetrates the material of interest and the non-absorbed energy is diffusely reflected from the sample. The reflected energy is collected by PbS (lead sulfide) detectors and is used to quantify the extent of absorption at each wavelength. Both sides of each tablet sample were scanned, except for flat-faced tablets, which had one side scanned. Each reflectance spectrum was recorded using Vision software (Foss NIRSystems Inc., Laurel, MD, USA) by integrating 32 scans taken from 1100 to 2450 nm at 0.5 nm intervals. A reference (a ceramic plate) spectrum was obtained previously, in order to compute each tablet's reflectance spectrum.

After obtaining spectra with the reflectance technique, the same tablet samples were analyzed using an InTact MultiTab Analyzer (Foss NIRSystems Inc., Laurel, MD, USA). The InTact MultiTab analyzer is specifically designed to analyze tablets using the transmittance NIR spectroscopic technique. The light transmitted through the tablets is then measured using a sensitive InGaAs (indium gallium arsenide) detector positioned immediately beneath the tablet. A tablet auto-sampler with 30 templates, which closely fits the contour of the tablets and has an aperture (Ø 6.0 mm) beneath the tablet, is used as a sample holder in order to avoid producing an undesired mixed-mode, i.e. combined transmittance and reflectance, spectrum due to stray light or light leakage. The template also ensures consistent sample presentation to the instrument, and this minimizes a significant source of the measurement variability. Both sides of each tablet sample were scanned, except for flat-faced tablets, which had one side scanned. Each transmittance spectrum was recorded using Vision software by integrating 32 scans taken from 800 to 1300 nm at 2 nm intervals. A reference (ambient air) spectrum was obtained previously, in order to compute each tablet's transmittance spectrum.

### 2.4. HPLC analysis

After the collection of all the spectra from each individual tablet, the reference HPLC analysis was performed. First, each individual tablet was transferred to a 200-ml volumetric flask. After adding about 140 ml of diluent (purified water–acetonitrile (25:3, v/v)), the flask was vibrated with occasional shaking in an ultrasonic bath (BRANSON model 8510 Ultrasonic Cleaner, Branson Ultrasonic Corporation, Danbury, CT, USA) until the tablet had disintegrated and the mixture was then diluted to volume with the diluent. A part of the content of the flask was transferred to a centrifuging tube and was centrifuged for 5 min at 3000 rpm. Two milliliters of the resulting supernatant solution and 5 ml of internal standard solution (1 mg/ml salicylic acid solution diluted by the diluent) were both pipetted into a 50-ml volumetric flask and diluted to volume with the diluent.

Separately, 120 mg of caffeine anhydrate was accurately weighed into a 200-ml volumetric flask and the same operation described above was carried out to prepare standard solution.

The samples were then analyzed by HPLC with UV detection. The HPLC system consisted of an LC-10AD pump in combination with an SIL-10A auto-injector (Shimadzu Corporation, Kyoto, Japan). An L-Column ODS (5 μm, 250 mm × 4.6 mm i.d.) from the Chemicals Evaluation and Research Institute (Tokyo, Japan) was used. Detection at 280 nm was carried out with an SPD-10A UV/Vis Detector from Shimadzu Corporation (Kyoto, Japan). The mobile phase was phosphate buffer (pH 4.0; 0.05 M)–acetonitrile (25:3, v/v) with a

**Table 2**
Batch analysis results

| Batch no. | n | Tablet weight (mg) | | Tablet thickness (mm) | | API content (HPLC, mg) | |
|---|---|---|---|---|---|---|---|
| | | Mean | S.D. | Mean | S.D. | Mean | S.D. |
| 1 | 3 | 299.9 | 0.2 | 3.25 | 0.01 | 89.1 | 0.7 |
| 2 | 3 | 300.1 | 0.4 | 3.23 | 0.02 | 92.1 | 0.9 |
| 3 | 3 | 300.4 | 0.2 | 3.24 | 0.02 | 101.3 | 0.1 |
| 4 | 3 | 300.0 | 0.4 | 3.25 | 0.03 | 107.3 | 1.6 |
| 5 | 3 | 300.2 | 0.1 | 3.26 | 0.02 | 114.1 | 0.9 |
| 6 | 3 | 300.4 | 0.3 | 3.24 | 0.02 | 119.7 | 0.8 |
| 7 | 3 | 300.3 | 0.1 | 3.26 | 0.01 | 126.0 | 0.2 |
| 8 | 3 | 300.4 | 0.2 | 3.24 | 0.02 | 131.7 | 0.6 |
| 9 | 3 | 300.4 | 0.2 | 3.26 | 0.02 | 138.7 | 0.8 |
| 10 | 3 | 300.3 | 0.4 | 3.40 | 0.02 | 94.4 | 0.2 |
| 11 | 3 | 300.4 | 0.2 | 3.14 | 0.01 | 93.7 | 0.5 |
| 12 | 3 | 300.2 | 0.3 | 3.10 | 0.01 | 95.0 | 0.5 |
| 13 | 3 | 300.1 | 0.4 | 3.04 | 0.01 | 95.0 | 0.8 |
| 14 | 3 | 300.3 | 0.4 | 3.44 | 0.01 | 113.7 | 1.8 |
| 15 | 3 | 300.3 | 0.1 | 3.15 | 0.03 | 113.4 | 0.4 |
| 16 | 3 | 300.1 | 0.2 | 3.11 | 0.01 | 115.2 | 0.6 |
| 17 | 3 | 300.1 | 0.6 | 3.06 | 0.01 | 114.3 | 0.6 |
| 18 | 3 | 300.7 | 0.1 | 3.40 | 0.02 | 132.1 | 0.1 |
| 19 | 3 | 300.3 | 0.4 | 3.16 | 0.02 | 131.7 | 1.5 |
| 20 | 3 | 300.8 | 0.5 | 3.10 | 0.01 | 132.5 | 1.1 |
| 21 | 3 | 300.4 | 0.3 | 3.05 | 0.02 | 132.5 | 0.5 |
| 22 | 3 | 300.5 | 2.3 | 3.31 | 0.02 | 93.6 | 0.9 |
| 23 | 3 | 299.9 | 1.0 | 3.31 | 0.01 | 112.8 | 0.7 |
| 24 | 3 | 301.1 | 0.8 | 3.33 | 0.01 | 132.0 | 0.6 |
| 25 | 3 | 300.3 | 2.0 | 4.38 | 0.01 | 95.0 | 1.8 |
| 26 | 3 | 300.3 | 1.0 | 4.37 | 0.01 | 112.8 | 0.6 |
| 27 | 3 | 300.5 | 0.6 | 4.38 | 0.01 | 129.5 | 0.2 |
| 28 | 5 | 300.3 | 0.3 | 3.42 | 0.01 | 119.3 | 0.6 |
| 29 | 5 | 300.6 | 0.3 | 3.16 | 0.01 | 119.6 | 0.9 |
| 30 | 5 | 300.9 | 0.5 | 3.32 | 0.00 | 120.2 | 1.2 |
| 31 | 5 | 300.7 | 0.8 | 4.38 | 0.00 | 119.2 | 0.6 |
| 32 | 5 | 300.4 | 0.3 | 3.25 | 0.02 | 120.3 | 0.5 |

flow rate of 1.0 ml/min. Chromatograms were collected and integration took place using a Chromatopack from Shimadzu Corporation (Kyoto, Japan). The API contents calculated were expressed as mg per tablet (Table 2) because this has been shown to lower the prediction error in PLS regression compared to mg per weight or mg per volume of the tablet [36].

### 2.5. Spectral analysis and generation of calibration models

The raw spectral data were first converted to the second derivative data (segment size = 20 nm, gap = 0) using Vision software, in order to remove the baseline offset and sloping effects that are common in NIR spectra. Calibration models were generated by PLS using the second derivative spectral data obtained from both the reflectance and transmittance techniques. The criterion for selecting the number of PLS factors was based on the prediction residual error-sum of squares (PRESS) by a leave-one-out cross-validation performed with the Vision software. The wavelength ranges of the spectral data used to generate the PLS calibration models for the reflectance and the transmittance techniques were 1100–2450 and 800–1300 nm, respectively.

The calibration models were then used to predict the API content of the intact tablets and to assess the effect of the tablet thickness, shape, embossing and scored line on the predicted API content. To assess the effect of the tablet thickness on the predicted API content, the root mean square-error of prediction (RMSEP) of the tablets compressed by 6.5, 9.0 and 11.5 kN forces (batch nos. 28, 32 and 29 in Table 1) were evaluated. To assess the effect of the tablet shape on the predicted API content, the RMSEP of flat-faced, flat beveled edge and convex tablets (batch nos. 32, 30 and 31 in Table 1) using the spectra scanned on the smooth side of the tablets were evaluated. The RMSEP is defined as follows:

$$\mathrm{RMSEP} = \sqrt{\frac{\sum_{i=1}^{n}(y_i - Y_i)^2}{n}}$$

where $n$ is the number of samples, $y$ is the API content by HPLC and $Y$ is the API content by NIR. The guidance issued by European Agency [39] recommends that the RMSEP should be smaller than the 1.4 times of the allowed error in the HPLC method. Therefore, the criterion for acceptable predictability for the various designed tablets was RMSEP $\leq$ 1.7 because the allowed error in the reference HPLC method in this study was 1.2. To assess the effect of the surface shape of tablets on the predicted API content, the differences in the API content values predicted from the spectra scanned on the smooth side and embossed (and scored) side of the tablets (batch nos. 30 and 31 in Table 1) were calculated.

## 3. Results and discussion

### 3.1. Spectral changes by variations in API content, tablet thickness and shape

First, the NIR spectral changes in terms of variations in the API content of the tablets were examined. As the API content of the tablets increased, the intensities of the bands at 1670, 1720, 2250 and 2430 nm increased (second derivative value decreased) in the reflectance spectra (Fig. 2(a)), and those of the bands at 890, 990, 1120 and 1170 nm increased in the transmittance spectra (Fig. 2(b)). Since these bands correspond to the wavelengths of the second derivative spectrum peaks of caffeine anhydrate, these changes reflect the variations in the API content of the tablets.

Fig. 3 shows the changes of the second derivative spectra in terms of variations in the tablet thickness (3.0–3.5 mm) obtained

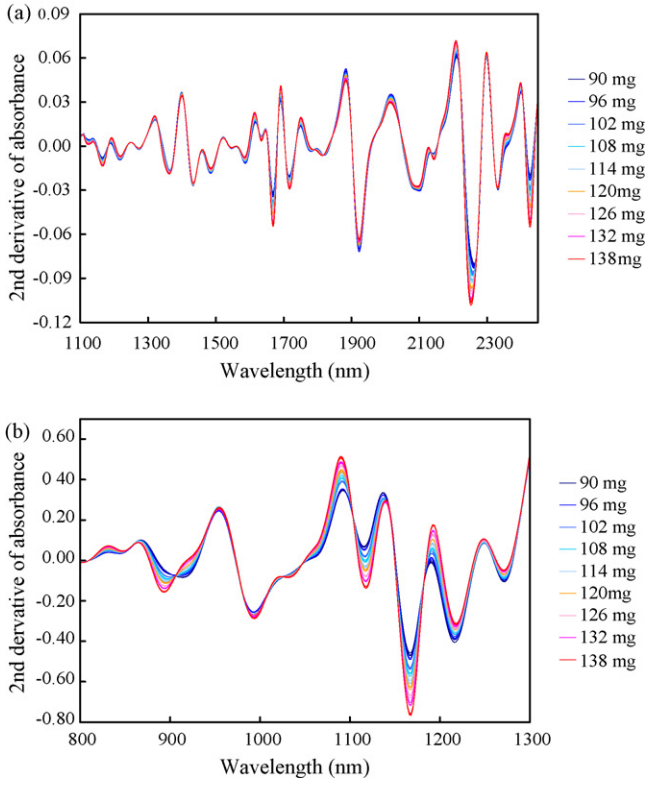


**Fig. 2.** Variation of near-infrared second derivative spectra of flat-faced tablets with their API content ($n$ = 3): (a) reflectance and (b) transmittance.

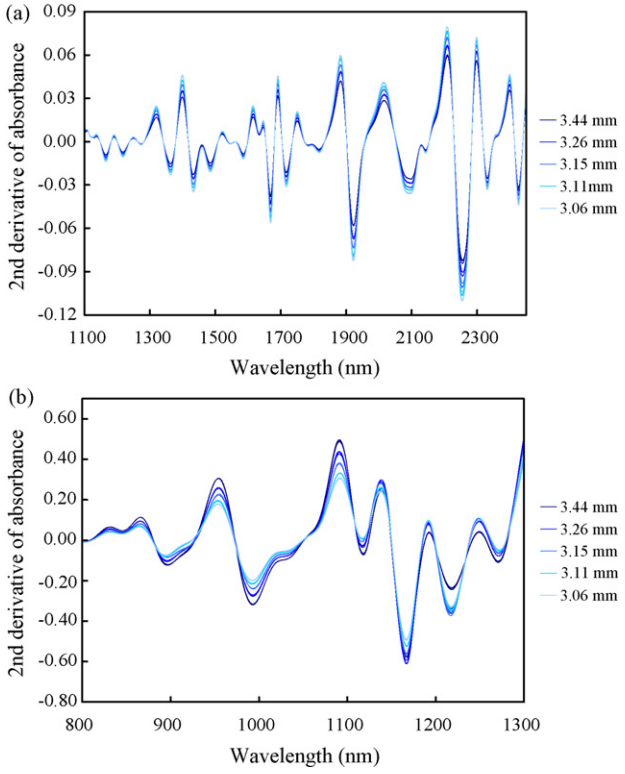


**Fig. 3.** Variation of near-infrared second derivative spectra of flat-faced tablets with their thickness ($n = 3$): (a) reflectance and (b) transmittance.

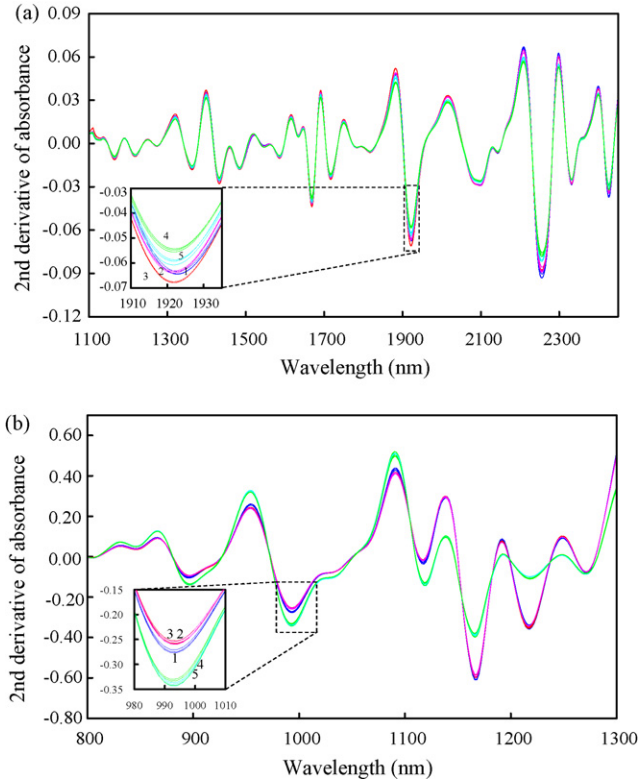


**Fig. 4.** Near-infrared second derivative spectra of tablets with various designs obtained by scanning both sides of the tablets ($n = 3$): (a) reflectance and (b) transmittance. (Blue line, 1) Flat-faced; (pink line, 2) flat beveled edge (smooth side); (red line, 3) flat beveled edge (embossed and scored side); (green line, 4) convex (smooth side); (light blue line, 5) convex (embossed side). (For interpretation of the references to color in this figure legend, the reader is referred to the web version of the article.)

from both the reflectance (Fig. 3(a)) and transmittance (Fig. 3(b)) techniques. As the tablet thickness decreased (tablet density increased), the intensities of each peak in the reflectance spectra increased. This is attributed to the decrease in the multiple scattering of light in the tablets and the relative increase in the penetration depth into the tablets due to tablet densification, i.e. increase in the absorption of the irradiated light [34,35]. On the contrary, as tablet thickness decreased, the intensities of each peak in the transmittance spectra decreased. This is attributed to the decrease of the light path length in the tablets caused by the reduction of the tablet height and the increase in the straight light path ratio [34,35] in the tablets.

Fig. 4 shows the second derivative spectra of the various designed tablets obtained by scanning both the smooth side and the embossed (and scored) side using both the reflectance (Fig. 4(a)) and transmittance (Fig. 4(b)) techniques. As for the reflectance spectra, there were differences among the tablet shapes and differences depending on scanned sides of the tablets. These results are probably caused by the difference in the scattering of the irradiated light on the rounded surface, embossing or scored line. As for the transmittance spectra, similar spectra were obtained from the smooth side and embossed (and scored) side of each tablet, but considerable differences were noted among the different tablet shapes, especially in the longer wavelengths of the convex tablet. These results are probably attributed to differences in the extent of the scattering of irradiated light inside the tablets, that is, the degree of absorption at certain wavelengths changes due to changes in the light path length.

### 3.2. Effect of tablet thickness and shape on predicted API content

Calibration models were generated by PLS using the second derivative spectral data (as *X* matrices) and the corresponding HPLC reference values (as *Y* matrices) of tablets prepared at a fixed compression force with the flat-faced punches (batch nos. 1–9). Then the prediction of the API content in the tablets was performed to assess the effect of tablet thickness (batch nos. 28, 29 and 32) and shape (batch nos. 30 and 31, using only the spectra for the smooth side) on the predicted API content. The calibration and prediction results are summarized in Table 3. The PLS factors used in the reflectance model and the transmittance model were 1 and 3,

**Table 3**
Prediction results; calibration set (variables): API content

| Batch no. | ID no. | | | | | Mean | S.D. | RMSEP |
|---|---|---|---|---|---|---|---|---|
| | 1 | 2 | 3 | 4 | 5 | | | |
| Predicted value (mg) | | | | | | | | |
| Reflectance | | | | | | | | |
| 32 | 120.3 | 120.7 | 118.5 | 122.6 | 117.9 | 120.0 | 1.9 | 1.9 |
| 28 | 110.3 | 113.9 | 113.0 | 107.8 | 109.8 | 111.0 | 2.4 | 8.6 |
| 29 | 123.7 | 122.9 | 127.4 | 125.9 | 126.7 | 125.3 | 1.9 | 6.0 |
| 30 | 117.5 | 119.1 | 118.3 | 118.2 | 116.0 | 117.8 | 1.2 | 2.4 |
| 31 | 107.6 | 108.1 | 107.0 | 105.5 | 104.4 | 106.5 | 1.5 | 12.7 |
| Transmittance | | | | | | | | |
| 32 | 119.7 | 119.6 | 118.6 | 119.5 | 119.9 | 119.5 | 0.5 | 1.1 |
| 28 | 122.7 | 122.8 | 122.8 | 123.2 | 123.6 | 123.0 | 0.4 | 3.8 |
| 29 | 117.5 | 116.6 | 117.7 | 118.8 | 116.0 | 117.3 | 1.1 | 2.6 |
| 30 | 118.7 | 118.5 | 118.2 | 117.8 | 117.9 | 118.2 | 0.4 | 2.3 |
| 31 | 129.9 | 128.7 | 127.2 | 127.3 | 127.7 | 128.1 | 1.1 | 8.9 |

Reflectance model: PLS factor, 1; correlation coefficient, 0.9927; SEC, 2.0; SECV, 2.1.
Transmittance model: PLS factor. 3; correlation coefficient, 0.9989; SEC, 0.8; SECV, 0.9.

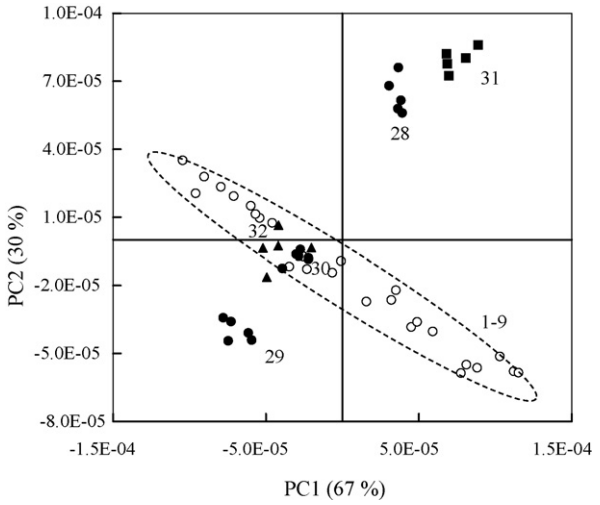


**Fig. 5.** Score plot from second derivative reflectance spectra by principal component analysis. Open symbols—calibration set: (○) flat-faced tablets with various content; closed symbols—prediction set: (●) flat-faced tablets with various thickness, (▲) flat beveled edge tablet, (■) convex tablet. The numbers by the data points correspond to the batch no. in Table 1. Explained *X*-variance, PC1: 0.67, PC2: 0.30, PC3: 0.02.

respectively. The standard error of calibration (SEC) was 2.0 and 0.8, the standard error of cross-validation (SECV) was 2.1 and 0.9, for the reflectance model and the transmittance model, respectively.

The prediction results of the tablets with different thicknesses gave large RMSEPs with both of the techniques. In the same way, the prediction results of the tablets with different shapes also gave large RMSEPs with both of the techniques. Hence, the prediction of the API content in tablets was strongly affected by the tablet thickness and shape using either of the techniques with calibration sets which consist of tablets of fixed thickness and shape. An additional remark which should be made here is that when using the transmittance technique, the RMSEPs of different thicknesses or shapes were smaller than that when using the reflectance technique, whereas the spectral differences between tablet thickness or shapes using the transmittance technique seemed to be equal to or larger than those using the reflectance technique (Figs. 3 and 4). The reason for this phenomenon is discussed below.

Figs. 5 and 6 show the score plots derived from principal component analyses of the second derivative spectral data obtained using the reflectance technique and the transmittance technique, respectively. The plots of batch nos. 28, 29 and 31 in the reflectance technique and batch nos. 28 and 31 in the transmittance technique were considerably out of the distribution of each calibration set. Generally, the API contents in the tablets out of the calibration sets, i.e. outliers, are predicted inaccurately. The similarity of the prediction samples to the calibration set can be determined by the Mahalanobis distance. The Mahalanobis distance is defined as follows:

$$D_i^2 = (x_i - \bar{x}_j)S^{-1}(x_i - \bar{x}_j)'$$

with

$$S = \frac{1}{n-1}\sum_{i=1}^{n}(x_i - \bar{x}_j)'(x_i - \bar{x}_j)$$

where $x_i$ is the vector of each sample, $\bar{x}_j$ is the mean vector, $n$ is the number of samples and $S$ is the variance–covariance matrix. That is, the Mahalanobis distance takes into account the covariance among the variables in calculating distances and is a useful way of determining the similarity of the prediction samples to the calibration set.

**Table 4**
Two-dimensional (PC1 and PC2) Mahalanobis distances of prediction samples ($n = 5$) to the center of each calibration set

| | Batch no. | Reflectance | | Transmittance | |
|---|---|---|---|---|---|
| | | Mean | S.D. | Mean | S.D. |
| Flat-faced tablets | | | | | |
| Pressure: 9.0 kN | 32 | 2.0 | 3.2 | 0.6 | 0.4 |
| Pressure: 6.5 kN | 28 | 314.8 | 52.7 | 248.8 | 27.0 |
| Pressure: 11.5 kN | 29 | 106.8 | 15.7 | 2.1 | 0.6 |
| Flat beveled edge tablet | 30 | 5.2 | 7.7 | 3.4 | 3.4 |
| Convex tablet | 31 | 569.1 | 75.0 | 495.8 | 66.4 |

The Mahalanobis distances of the prediction samples to the center of the correspondent calibration set are shown in Table 4. The Mahalanobis distances of each sample using the transmittance technique were shorter than those using the reflectance technique, that is, the deviation from the distribution of the calibration set was relatively small using the transmittance technique. This suggests that the transmittance spectra reflect the differences in tablet thickness or shape as a result of obtaining information inside the tablets even if they are prepared at fixed compression force with the flat-faced punches. This is why the RMSEPs of tablets with different thicknesses or shapes were smaller when the transmittance technique was applied.

### 3.3. Effect of embossing and scored line on predicted API content

Adding the tablet thickness (batch nos. 10–21) and shape (batch nos. 22–27, using only the spectra for the smooth side) variations to the models given above provided calibration models with SECs of 1.7 and 0.9, SECVs of 2.0 and 1.0, for the reflectance technique and the transmittance technique, respectively. The PLS factors used in the reflectance model and the transmittance model were 7 and 9, respectively. By using these models, the effects of tablet thickness, shape, embossing and scored line on the predicted value were assessed. The calibration and prediction results are summarized in Table 5.

Prediction of the API content in tablets was scarcely affected by the tablet thickness or shape using both of the techniques. This

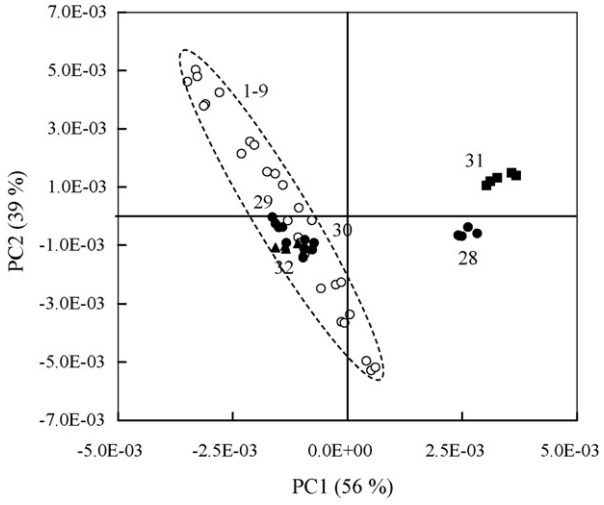


**Fig. 6.** Score plot from second derivative transmittance spectra by principal component analysis. Open symbols—calibration set: (○) flat-faced tablets with various content; closed symbols—prediction set: (●) flat-faced tablets with various thickness, (▲) flat beveled edge tablet, (■) convex tablet. The numbers by the data points correspond to the batch no. in Table 1. Explained *X*-variance, PC1: 0.56, PC2: 0.39, PC3: 0.04.

**Table 5**
Calibration and prediction results; calibration set (variables): API content, tablet thickness and tablet shape

| Batch no. | Scan side | ID no. | | | | | Mean | S.D. | RMSEP |
|---|---|---|---|---|---|---|---|---|---|
| | | 1 | 2 | 3 | 4 | 5 | | | |
| Predicted value (mg) | | | | | | | | | |
| Reflectance | | | | | | | | | |
| 32 | Smooth | 119.4 | 118.4 | 117.2 | 118.6 | 118.6 | 118.4 | 0.8 | 2.1 |
| 28 | Smooth | 121.5 | 122.7 | 121.6 | 121.9 | 117.1 | 121.0 | 2.2 | 2.6 |
| 29 | Smooth | 122.7 | 119.4 | 119.8 | 123.3 | 121.6 | 121.4 | 1.7 | 2.5 |
| 30 | Smooth | 119.5 | 118.5 | 118.2 | 118.6 | 118.2 | 118.6 | 0.5 | 2.1 |
| 31 | Smooth | 120.0 | 115.3 | 119.0 | 115.8 | 115.6 | 117.1 | 2.2 | 2.6 |
| 30 | Embossed and scored | 122.5 | 124.6 | 115.6 | 114.9 | 124.1 | 120.4 | 4.7 | 4.7 |
| 31 | Embossed | 116.2 | 117.3 | 117.7 | 119.6 | 119.0 | 118.0 | 1.4 | 2.1 |
| Transmittance | | | | | | | | | |
| 32 | Smooth | 119.7 | 119.3 | 119.9 | 120.0 | 120.3 | 119.8 | 0.4 | 0.8 |
| 28 | Smooth | 120.5 | 121.0 | 120.6 | 120.3 | 120.5 | 120.6 | 0.3 | 1.4 |
| 29 | Smooth | 120.8 | 119.3 | 119.7 | 119.9 | 121.9 | 120.3 | 1.1 | 1.4 |
| 30 | Smooth | 120.8 | 120.6 | 120.7 | 120.5 | 120.6 | 120.6 | 0.1 | 1.2 |
| 31 | Smooth | 119.0 | 118.4 | 119.5 | 120.6 | 119.7 | 119.4 | 0.8 | 1.1 |
| 30 | Embossed and scored | 120.8 | 119.1 | 120.1 | 120.1 | 120.2 | 120.1 | 0.6 | 1.6 |
| 31 | Embossed | 119.2 | 119.3 | 119.0 | 119.6 | 119.1 | 119.2 | 0.2 | 0.6 |
| Absolute value of difference between scan sides (mg) | | | | | | | | | |
| Reflectance | | | | | | | | | |
| 30 | – | 3.1 | 6.2 | 2.6 | 3.7 | 6.0 | 4.3 | 1.7 | |
| 31 | – | 3.8 | 2.0 | 1.3 | 3.8 | 3.4 | 2.9 | 1.2 | |
| Transmittance | | | | | | | | | |
| 30 | – | 0.1 | 1.5 | 0.6 | 0.5 | 0.4 | 0.6 | 0.6 | |
| 31 | – | 0.2 | 0.9 | 0.5 | 1.0 | 0.6 | 0.7 | 0.3 | |

Reflectance model: PLS factor, 7; correlation coefficient, 0.9942; SEC, 1.7; SECV, 2.0. Transmittance model: PLS factor, 9; correlation coefficient, 0.9984; SEC, 0.9; SECV, 1.0.

is probably attributed to the incorporation of the distribution due to variations in the tablet thickness and shape (Figs. 5 and 6) into the calibration models. In particular, the effect of these elements on the predicted value using the transmittance model was smaller and this is probably because the transmittance spectra can sensitively reflect differences in the tablets, such as tablet thickness or shape. Embossing and scored line, especially scored line on the flat beveled edge tablets, affected API content prediction only when using the reflectance technique, since the irradiated light was influenced by the embossing and scored line. The reason why the scored

**Table 6**
Calibration and prediction results; calibration set (variables): API content, tablet thickness, tablet shape and surface shape

| Batch no. | Scan side | ID no. | | | | | Mean | S.D. | RMSEP |
|---|---|---|---|---|---|---|---|---|---|
| | | 1 | 2 | 3 | 4 | 5 | | | |
| Predicted value (mg) | | | | | | | | | |
| Reflectance | | | | | | | | | |
| 32 | Smooth | 119.3 | 118.3 | 117.6 | 118.5 | 118.6 | 118.5 | 0.6 | 2.0 |
| 28 | Smooth | 121.6 | 122.8 | 121.7 | 122.2 | 117.5 | 121.1 | 2.1 | 2.6 |
| 29 | Smooth | 122.3 | 119.1 | 119.9 | 122.9 | 121.0 | 121.0 | 1.6 | 2.2 |
| 30 | Smooth | 118.8 | 118.0 | 117.7 | 118.4 | 117.9 | 118.1 | 0.4 | 2.5 |
| 31 | Smooth | 119.1 | 116.4 | 117.4 | 116.5 | 116.4 | 117.2 | 1.2 | 2.2 |
| 30 | Embossed and scored | 121.5 | 123.4 | 120.2 | 119.0 | 123.2 | 121.5 | 1.9 | 2.5 |
| 31 | Embossed | 117.3 | 117.9 | 118.7 | 119.4 | 118.9 | 118.4 | 0.9 | 1.5 |
| Transmittance | | | | | | | | | |
| 32 | Smooth | 119.7 | 119.4 | 119.9 | 120.0 | 120.4 | 119.9 | 0.4 | 0.8 |
| 28 | Smooth | 120.8 | 121.3 | 120.9 | 120.6 | 120.7 | 120.9 | 0.3 | 1.7 |
| 29 | Smooth | 121.0 | 119.5 | 119.9 | 120.0 | 122.1 | 120.5 | 1.1 | 1.5 |
| 30 | Smooth | 121.3 | 121.0 | 121.2 | 121.1 | 121.1 | 121.2 | 0.1 | 1.5 |
| 31 | Smooth | 118.9 | 118.2 | 119.6 | 120.8 | 119.8 | 119.5 | 1.0 | 1.2 |
| 30 | Embossed and scored | 121.5 | 119.6 | 120.8 | 120.8 | 120.9 | 120.7 | 0.7 | 1.7 |
| 31 | Embossed | 119.1 | 119.2 | 119.0 | 119.7 | 119.1 | 119.2 | 0.3 | 0.6 |
| Absolute value of difference between scan sides (mg) | | | | | | | | | |
| Reflectance | | | | | | | | | |
| 30 | – | 2.8 | 5.4 | 2.5 | 0.6 | 5.3 | 3.3 | 2.0 | |
| 31 | – | 1.9 | 1.5 | 1.3 | 2.9 | 2.5 | 2.0 | 0.7 | |
| Transmittance | | | | | | | | | |
| 30 | – | 0.2 | 1.4 | 0.4 | 0.3 | 0.2 | 0.5 | 0.5 | |
| 31 | – | 0.2 | 1.0 | 0.6 | 1.2 | 0.7 | 0.7 | 0.4 | |

Reflectance model: PLS factor, 7; correlation coefficient, 0.9941; SEC, 1.7; SECV, 2.0. Transmittance model: PLS factor, 9; correlation coefficient, 0.9985; SEC, 0.9; SECV, 0.9.

line exhibited the largest effect is that it has considerable depth and exists in the center of tablets where the irradiated light is mainly provided. On the contrary, with the transmittance technique, embossing and scored line scarcely affected the API content prediction because the degree of transmission of irradiated light was hardly influenced by the surface shape variation of each tablet (Fig. 4).

Aiming for incorporation of the surface shape variation into the calibration models, the same approach as mentioned above was applied to the cancellation of the surface shape variation effect. Adding the surface shape; embossing and scored line variations (batch nos. 22–27, using the spectra scanned on the embossed (and scored) side of the tablets) to the reflectance model provided a calibration model with seven PLS factors, SEC of 1.7 and SECV of 2.0, by which the effect of the surface shape variations on the predicted value was reduced. The calibration and prediction results are summarized in Table 6. On the other hand, adding these variations to the transmittance model scarcely improved its predictability with regard to surface shape variations (Table 6). However, the effect of the surface shape variations on the predicted value using the reflectance model was still larger than that using the transmittance model. This result suggests that the reflectance technique is not suitable for tablets with embossing and scored line.

### 3.4. Validation and comparison of the reflectance and transmittance model

From the above-mentioned results, the reflectance model with tablet thickness and shape variations including surface shape variations (Table 6) and the transmittance model with tablet thickness and shape variations (Table 5) were adopted and the method validation of each model was carried out.

Specificity can be explained using the loadings for the PLS factors used. Each of the loading vectors of PLS factor 1 in the reflectance and transmittance models resembled the second derivative spectrum of API (data not shown). Therefore, each of the PLS factor 1 contains information on the API content and these models specifically quantify the API content.

The linearity and accuracy of these models are summarized in Table 7. The linearity and accuracy of the transmittance model were superior to those of the reflectance model. In particular, the SECV of the transmittance model was 1.0 and this was equivalent to the allowed error for the reference HPLC method, in which the maximum allowed error was 1.2. This superior accuracy was also supported by the fact that the PRESS using the transmittance model was smaller than that using the reflectance one over two PLS factors (Fig. 7). These results could possibly be due to the fact that the transmittance technique analyzes almost the entire tablet, whereas the reflectance technique analyzes only the tablet's surface layer

**Table 7**
Validation results of the reflectance and transmittance models

| Parameters | Results | |
|---|---|---|
| | Reflectance | Transmittance |
| Linearity | | |
| Content range | 88.5–139.6 | 88.5–139.6 |
| Correlation coefficient | 0.9941 | 0.9985 |
| *Y*-intercept | 1.3 | 0.3 |
| Slope of calibration line | 0.9883 | 0.9971 |
| Accuracy | | |
| SEC | 1.7 | 0.9 |
| SECV | 2.0 | 1.0 |
| Average difference of prediction set | 0.1 | 0.0 |
| PRESS | 548.1 | 130.2 |

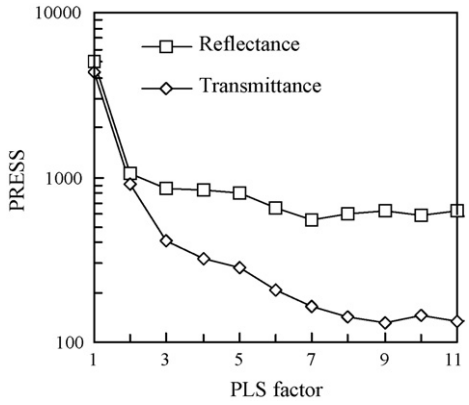


**Fig. 7.** Variation of prediction residual error-sum of squares (PRESS) with the number of the PLS factor.

[37]. Hence, the predicted values obtained using the reflectance technique are more sensitive to the distribution of API content in the tablet. This may account for the results obtained using the transmittance technique being closer to the API content values determined by the HPLC reference method than those obtained using the reflectance technique. Thus, the transmittance model quantifies the API content in the tablets more accurately than the reflectance model.

From these results, the transmittance model is suitable as an assay method which is readily applicable to various designed tablets.

## 4. Conclusions

The effect of such elements of tablet design as thickness, shape, embossing and scored line on the NIR spectra and API content measurement in tablets containing caffeine anhydrate was examined using the reflectance and transmittance techniques. The tablet thickness, shape, embossing and scored line affected the reflectance spectra; the tablet thickness and shape affected the transmittance spectra. Therefore, the prediction of the drug content was affected by these elements when using calibration models generated with a fixed design according to the conventional calibration method using each of these techniques. As a result, these calibration models were hardly applicable to various designed tablets.

On the other hand, when variables regarding tablet design were included in the model, the prediction of the API content in the tablets was scarcely affected by elements such as tablet thickness, shape, embossing and scored line using either of the techniques. In order to obtain such versatile model, the reflectance model needed variations in all the elements relating to the tablet design, though the transmittance one needed only to take the tablet thickness and shape into consideration. A comparison of these techniques demonstrated higher predictability under the tablet design variations using the transmittance technique with preferable linearity and accuracy because the transmittance spectra can sensitively reflect differences in the tablets, such as tablet thickness or shape. The linearity and accuracy could be possibly due to the fact that the transmittance technique analyzes almost the entire tablet.

In conclusion, utilizing transmittance NIR spectroscopy, an assay method which is readily applicable to tablets with various designs was developed by adding variation factors which originate in the tablet design to the calibration model. This calibration model and its development method would be suitable for content measurement in tablets under development in which frequent changes in tablet design are made. As well, the application of this methodology to

pharmaceutical development would contribute to the progress of PAT.

## Acknowledgements

We would like to acknowledge NIRECO Corporation for the use of their NIR instruments and N. Fukutsu for his helpful discussions.

## References

[1] Food, Drug Administration, Guidance for Industry PAT—A Framework for Innovative Pharmaceutical Development, Manufacturing, and Quality Assurance, 2004.
[2] J. Rantanen, S. Lehtola, P. Rämet, J.P. Mannermaa, J. Yliruusi, Powder Technol. 99 (1998) 163–170.
[3] J. Rantanen, E. Rasanen, J. Tenhunen, M. Kansakoski, J. Mannermaa, J. Yliruusi, Eur. J. Pharm. Biopharm. 50 (2000) 271–276.
[4] A. Jorgensen, J. Rantanen, M. Karjalainen, L. Khriachtchev, E. Rasanen, J. Yliruusi, Pharm. Res. 19 (2002) 1285–1291.
[5] A.C. Jorgensen, P. Luukkonen, J. Rantanen, T. Schaefer, A.M. Juppo, J. Yliruusi, J. Pharm. Sci. 93 (2004) 2232–2243.
[6] T.D. Davis, G.E. Peck, J.G. Stowell, K.R. Morris, S.R. Byrn, Pharm. Res. 21 (2004) 860–866.
[7] W.P. Findlay, G.R. Peck, K.R. Morris, J. Pharm. Sci. 94 (2005) 604–612.
[8] A. Gupta, G.E. Peck, R.W. Miller, K.R. Morris, J. Pharm. Sci. 93 (2004) 1047–1053.
[9] A. Gupta, G.E. Peck, R.W. Miller, K.R. Morris, J. Pharm. Sci. 94 (2005) 1589–1597.
[10] D.J. Wargo, J.K. Drennen, J. Pharm. Biomed. Anal. 14 (1996) 1415–1423.
[11] S.S. Sekulic, J. Wakeman, P. Doherty, P.A. Hailey, J. Pharm. Biomed. Anal. 17 (1998) 1285–1309.
[12] A.S. El-Hagrasy, H.R. Morris, F. D'Amico, R.A. Lodder, J.K. Drennen III, J. Pharm. Sci. 90 (2001) 1298–1307.
[13] A.S. El-Hagrasy, F. D'Amico, J.K. Drennen III, J. Pharm. Sci. 95 (2006) 392–406.
[14] A.S. El-Hagrasy, M. Delgado-Lopez, J.K. Drennen III, J. Pharm. Sci. 95 (2006) 407–421.
[15] A.S. El-Hagrasy, J.K. Drennen, J. Pharm. Sci. 95 (2006) 422–434.
[16] O. Berntsson, L.G. Danielsson, B. Lagerholm, S. Folestad, Powder Technol. 123 (2002) 185–193.
[17] W. Li, M.C. Johnson, R. Bruce, S. Ulrich, H. Rasmussen, G.D. Worosila, Int. J. Pharm. 326 (2006) 182–185.
[18] W. Li, M.C. Johnson, R. Bruce, H. Rasmussen, G.D. Worosila, J. Pharm. Biomed. Anal. 43 (2007) 711–717.
[19] N.H. Duong, P. Arratia, F. Muzzio, A. Lange, J. Timmermans, S. Reynolds, Drug Dev. Ind. Pharm. 29 (2003) 679–687.
[20] P.E. Arratia, N. Duong, F.J. Muzzio, P. Godbole, A. Lange, S. Reynolds, Powder Technol. 161 (2006) 202–208.
[21] A.S. El-Hagrasy, S.Y. Chang, S. Kiang, Pharm. Dev. Technol. 11 (2006) 303–312.
[22] K.M. Morisseau, C.T. Rhodes, Pharm. Res. 14 (1997) 108–111.
[23] J.D. Perez-Ramos, W.P. Findlay, G. Peck, K.R. Morris, AAPS PharmSciTech 6 (2005) E127–E136.
[24] Y. Roggo, N. Jent, A. Edmond, P. Chalus, M. Ulmschneider, Eur. J. Pharm. Biopharm. 61 (2005) 100–110.
[25] G.E. Ritchie, R.W. Roller, E.W. Ciurczak, H. Mark, C. Tso, S.A. MacDonald, J. Pharm. Biomed. Anal. 29 (2002) 159–171.
[26] M. Laasonen, T. Harmia-Pulkkinen, C. Simard, M. Rasanen, H. Vuorela, Anal. Chem. 75 (2003) 754–760.
[27] M. Blanco, M. Alcala, J.M. Gonzalez, E. Torras, J. Pharm. Sci. 95 (2006) 2137–2144.
[28] M. Blanco, M. Alcala, Anal. Chim. Acta 557 (2006) 353–359.
[29] C.P. Meza, M.A. Santos, R.J. Romanach, AAPS PharmSciTech 7 (2006) E1–E9.
[30] B.V. Weiβner, J.-O. Henck, G. Reich, Proceedings of the Fifth World Meeting on Pharmaceutics, Biopharmaceutics and Pharmaceutical Technology, 2006.
[31] W. Li, A. Bashai-Woldu, J. Ballard, M. Johnson, M. Agresta, H. Rasmussen, S. Hu, J. Cunningham, D. Winstead, Int. J. Pharm. 340 (2007) 97–103.
[32] R. Mueller, P. Kleinebudde, Eur. J. Pharm. Biopharm. 64 (2006) 388–392.
[33] R. Mueller, P. Kleinebudde, Eur. J. Pharm. Biopharm. 67 (2007) 458–463.
[34] S. Tsuchikawa, S. Tsutsumi, Proceedings of the 9th International Conference on Near Infrared Spectroscopy, 2000, pp. 89–94.
[35] S. Tsuchikawa, in: S. Tsuchikawa (Ed.), Useful and Advanced Information in the Field of Near Infrared Spectroscopy, Research Signpost, Trivandrum, 2003, pp. 293–307.
[36] J. Gottfries, H. Depui, M. Fransson, M. Jongeneelen, M. Josefson, F.W. Langkilde, D.T. Witte, J. Pharm. Biomed. Anal. 14 (1996) 1495–1503.
[37] S.S. Thosar, R.A. Forbess, N.K. Ebube, Y. Chen, R.L. Rubinovitz, M.S. Kemper, G.E. Reier, T.A. Wheatley, A.J. Shukla, Pharm. Dev. Technol. 6 (2001) 19–29.
[38] M. Iyer, H.R. Morris, J.K. Drennen III, J. Near Infrared Spectrosc. 10 (2002) 233–245.
[39] The European Agency for the Evaluation of Medicinal Products, Note for Guidance on the Use pf Near Infrared Spectroscopy by the Pharmaceutical Industry and the Data Requirements for New Submissions and Variations, 2003.